Original Article

Exploration of the Development and Cell Communication of Aneuploid Osteoblasts and Osteoclasts in Giant Cell Tumour of Bone Using Single-Cell RNA Sequencing

(giant cell tumour of bone / single-cell RNA sequencing / osteoblasts / osteoclasts)

BO-HUA GAO, YAN WANG, YE ZHANG, ZHONG-REN CHEN, GUANG-FU MING

Department of Orthopedics, Hainan General Hospital (Hainan Affiliated Hospital of Hainan Medical University), China

Abstract. We aimed to explore the development and cell communication of osteoblasts and osteoclasts with aneuploidy variation in giant cell tumour of bone (GCTB). We predicted the diploid and aneuploid cells in tissue samples using the CopyKAT package. The Monocle2 package was used to analyse differentiation trajectories of aneuploid cells. We used the CellChat package to observe the signalling pathways and ligand-receptor pairs for the two interaction types, "Cell-Cell Contact" and "Secreted Signalling", respectively. A total of 9,117 cells were obtained including eight cell types. Most aneuploid cells were osteoblasts. As the cell differentiation trajectory matured, we found that aneuploid osteoblasts first increased the inflammatory response activity and then enhanced the ability to activate T cells, whereas osteoclasts gradually enhanced the cellular energy metabolism, cell adhesion, cell proliferation and immune response; the activated biological functions were gradually weakened. The analysis by CellChat indicated that *CTLA4* or *TIGIT* might act as important immune checkpoint genes to attenuate the inhibitory effect of aneuploid osteoclasts on NK/T cells, thereby enhancing the activity of NK/T cells. Our study found that both osteoblasts and osteoclasts might be involved in the development of GCTB, which may provide a new direction for the treatment of GCTB.

Received February 28, 2024. Accepted August 7, 2024.

Corresponding author: Guang-Fu Ming, Department of Orthopedics, Hainan General Hospital (Hainan Affiliated Hospital of Hainan Medical University), 19 Xiuhua Road, Xiuying district, Haikou, 570000, China. E-mail: mingguangfu2022@163.com

Abbreviations: CopyKAT – Copynumber Karyotyping of Tumors, DEGs – differentially expressed genes, GCTB – giant cell tumour of bone, GEO – Gene Expression Omnibus database, scRNA-seq – single-cell RNA sequencing, TME – tumour microenvironment, UMAP – uniform manifold approximation and projection.

Introduction

Giant cell tumour of bone (GCTB) is a rare neoplasm with the feature of locally aggressive lesions, which often occurs among the young adults in the ages of 30 and 40 years (Sbaraglia et al., 2021). Surgical resection is considered as the main treatment for GCTB. However, surgical resection is prone to local recurrence (in 20–50 %); repeated surgery after the initial surgery can lead to serious functional complications (van der Heijden et al., 2020). Recently, a report of Li and colleagues indicated that the drugs explored to decrease the role of osteoclasts, for example, denosumab and zoledronic acid, could lead to symptomatic relief but may not reduce the process of GCTB (Li et al., 2020). However, Giesche et al. (2022) proposed the osteoblast as the cell of origin of giant cell tumours of bone by using comparative methylation analysis. Thus, the deep understanding of the origin of osteoblasts and osteoclasts in GCTB plays an important role in clinical application.

In recent years, single-cell RNA sequencing (scRNA-seq) has demonstrated its potential value in exploring heterogeneity (Tirosh et al., 2016a; Mereu et al., 2020), inflammatory response and cell crosstalk within the tumour microenvironment (TME) across a variety of cancers (Tirosh et al., 2016b; Lee et al., 2020). Besides, it is universally known that aneuploidy occurs in nearly all cancers and is a hallmark of aging (Ji et al., 2021). Moskovszky et al. (2009) found that ploidy determination combined with FISH analysis might help predicting the recurrence potential of GCTB. When the body is induced to produce aneuploidy, it eventually leads to the death of apoptotic cancer cells (Yao et al., 2022). Thus, analysis and identification of aneuploid cells in GCTB may provide new directions for the treatment of patients.

Here, we first used CopyKAT to predict aneuploid cells and found that most aneuploid cells were osteoblasts. Next, we found by sub-subpopulation clustering and differentiation trajectory analysis of aneuploid osteoblasts that aneuploid osteoblasts enhance immune activation and reduce extracellular matrix production as they mature through differentiation and development.

Then, using sub-subgroup clustering and differentiation trajectory analysis of osteoclasts, we found that with the maturation of differentiation and development, osteoclasts gradually enhance the redox metabolism and decrease cell proliferation and immune response. Finally, through cell-to-cell communication analysis of cell contacts and secretory signals, we found that aneuploid osteoblasts activate NK/T cells via antigen presentation of the MHC family, and aneuploid osteoclasts suppress NK/T cells via TIGIT and CTLA4 NK/T cells.

Material and Methods

Collection and processing of scRNA-seq data

The scRNA-seq data with accession number GSE168664 (Feng et al., 2021) was downloaded from a Gene Expression Omnibus (GEO) database dataset including one GCTB sample. A total of 33,538 genes and 13,285 cells were obtained through production of a gene-barcode matrix using the Seurat package in R (version 4.1.2). We removed the cells of nFeature_RNA < 200 and mitochondrial gene ratio > 10 %. Furthermore, the DoubletFinder package was applied to remove potential double cells. Subsequently, a total of 9,117 cells were retained for the following analysis.

Clustering and annotation of cell types

The analysis of cell clustering and sub-clustering was performed using the FindClusters function in the Seurat package (resolution = 0.1). Identification of cell clusters and sub-clusters was carried out using uniform manifold approximation and projection (UMAP) analysis. We obtained the cell marker genes from the CellMarker database (Zhang et al., 2019) to annotate the sub-clustering cells.

Identification of aneuploid cells

CopyKAT (Copynumber Karyotyping of Tumors) identifies the genome-wide aneuploidies at 5MB resolution in single cells using the Bayesian approach and distinguishes tumour subclones based on high-throughput sc-RNA-seq data. Thus, to distinguish normal cells and malignant cells in the tumour microenvironment and to explore the subclonal structure inside the tumour, we applied the CopyKAT package (Gao et al., 2021) to predict the diploid cells and aneuploid cells in the GCTB sample. Notably, counting DNA copies requires at least five genes on each chromosome (ngene.chr = 5). Afterwards, the differentially expressed genes (DEGs) between aneuploid and diploid cells were identified using the FindMarker function with the threshold of |avg_log2_FC|>0.25 and p_val_adj < 0.05.

Pseudotime trajectory analysis

The Monocle2 package (Qiu et al., 2017) was used to analyse the differentiation trajectory of aneuploid osteoblasts and all osteoclasts and to observe the direction of differentiation of the sub-clustering cells with the threshold of mean expression > 0.1. We retained the DEGs with the q-value < 0.01 between the sub-clustering cells for dimension reduction using DDRTree of reduceDimension function. The plot_cell_trajectory() function was applied for ordering and visualizing the cells. After that, we calculated the DEGs with the q-value < $10^{\wedge -10}$ that changed along with the pseudotime, which were visualized using the plot_pseudotime_heatmap() function. The above-mentioned DEGs were divided into subgroups according to their expression patterns.

CellChat analysis

CellChat takes the gene expression data from cells as input and combines the ligand-receptor and its cofactor interactions to model cell-to-cell communication. In this study, we used it to explore the interaction ligand-receptor between aneuploidy variant osteoblasts or osteoclasts and NK/T cells, respectively. The CellChat package (Jin et al., 2021) was applied to study the interaction of Cell-Cell Contact and Secreted Signalling.

Statistical analysis

All statistical analyses and generation of pictures were performed using the R language (version 4.1.2). $P < 0.05$ was considered statistically significant.

Results

Most aneuploid cells in GCTB originate from osteoblasts

The 9,117 cells were clustered and visualized in Fig. 1A. Eight main types of cells were obtained, including mononuclear macrophages, osteoblasts, NK/T cells, osteoclasts, pericytes, proliferating cells, endothelial cells and chondrocytes. We listed the marker genes for the above cells as follows: *CD68*, *CD163*, *CD14* and *CSF1R* for mononuclear macrophages (Chen et al., 2020); *IBSP* and *RUNX2* for osteoblasts (Baird et al., 2018; Clark et al., 2019); *NKG7*, *CD3E* and *CD3D* for NK/T cells (Azizi et al., 2018; Peng et al., 2019; Zhou et al., 2020); *ACP5* and *CTSK* for osteoclasts (Nordstrand et al., 2018); *ACTA2* and *RGS5* for pericytes (Zhou et al., 2020); *MKI67*, *TOP2A* for proliferating cells (Liu et al., 2019); *PLVAP*, *EGFL7* for endothelial cells (Chim et al., 2011; Auvinen et al., 2019); *COL10A1*, *ACAN* for chondrocytes (Chen et al., 2019) (Fig. 1B).

After that, we used CopyKAT to identify diploid or aneuploid cells in the above-mentioned cells. As shown in Fig. 1C and 1D, we found that osteoblasts had the most aneuploid cells, up to 2,942. Following were endothelial cells, which contained 153 aneuploid cells; osteoclasts had 119 aneuploid cells.

Pseudotime trajectory analysis of aneuploid osteoblasts

Next, we analysed the pseudotime trajectory and subgrouping of aneuploid osteoblasts (Fig. 2A–D). We found

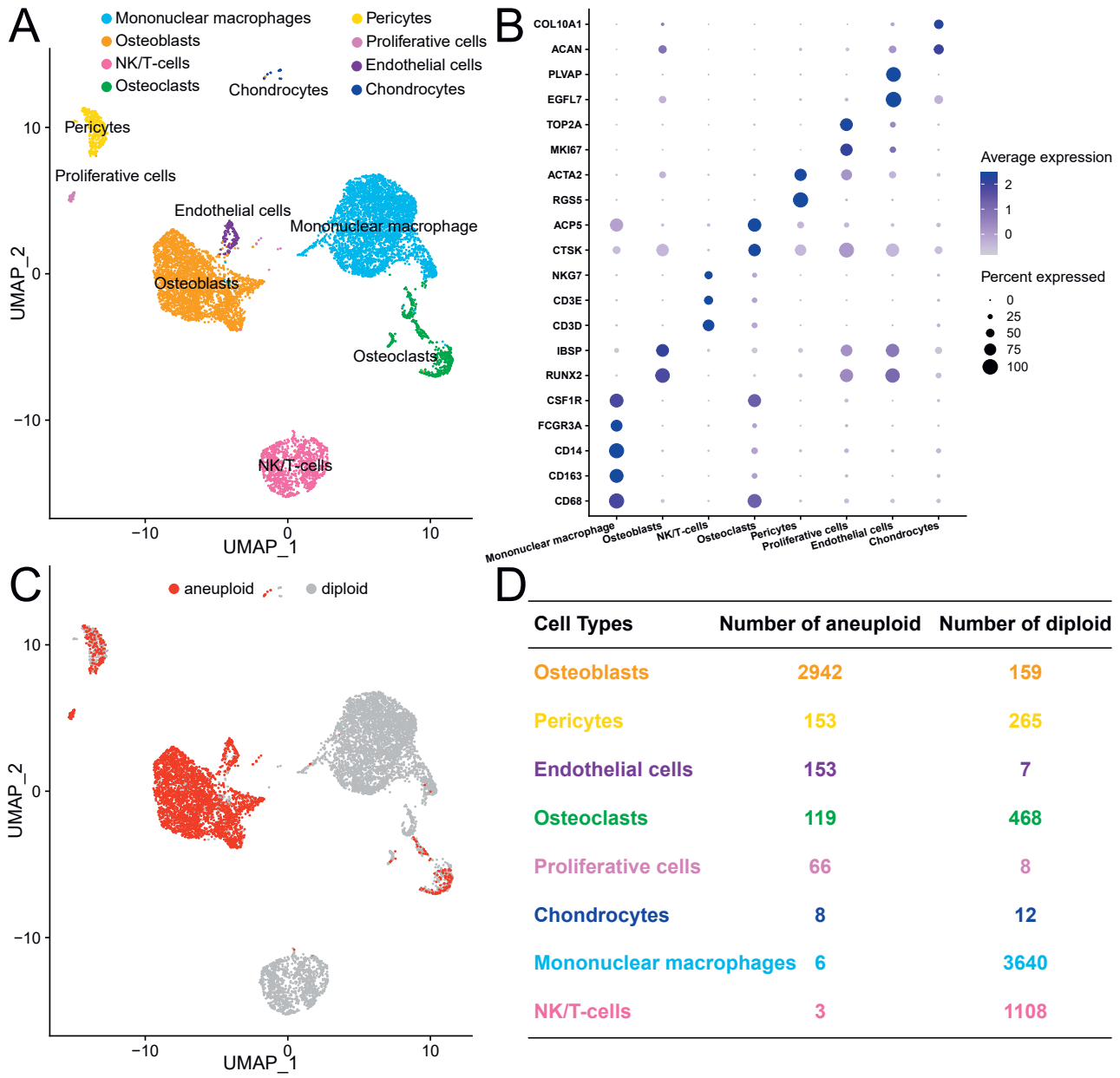

Cell Types	Number of aneuploid	Number of diploid
Osteoblasts	2942	159
Pericytes	153	265
Endothelial cells	153	7
Osteoclasts	119	468
Proliferative cells	66	8
Chondrocytes	8	12
Mononuclear macrophages	6	3640
NK/T-cells	3	1108

Fig. 1. scRNA-seq clustering analysis and aneuploid identification of GCTB. (**A**) UMAP plot of cell clustering and annotation. (**B**) Dot plot of canonical cellular markers of eight main cell types in GCTB. (**C**) UMAP plot of cells that are aneuploid or diploid. (**D**)The number of aneuploid and diploid cells in each cell type in GCTB.

that the aneuploid osteoblasts were divided into three clusters comprising C1_Osteoblasts, C2_Osteoblasts and C3_Osteoblasts (Fig. 2A). C2_Osteoblasts had a high expression level of *RUNX2* and *IBSP* (marker genes of mature osteoblasts) (Fig. 2B). Moreover, the pseudotime trajectory analysis indicated the maturation course of GCTB showing that the differentiation trajectory started with C1_Osteoblasts, developed to C3_Osteoblasts, which eventually differentiated into C2_Osteoblasts (Fig. 2C–D).

Then, the genes changed along with pseudotime were divided into three clusters. The gene expression value of Cluster 1 gradually increased with pseudotime, Cluster 2 showed a gradually decreasing trend with pseudotime, and Cluster 3 increased first and then decreased (Fig. 3A–D). Interestingly, the genes in Cluster 1 were involved in the T-cell functions such as T-cell activation, positive regulation of cell adhesion and lymphocyte immunity. Genes in Cluster 2 were enriched in the function of actin filaments, extracellular matrix including actin filament organization, regulation of actin filament-based process and muscle cell differentiation. Genes in Cluster 3 were mainly involved in inflammatory responses such as positive regulation of cytokine production, positive regulation of the response to external stimulus and cytoplasmic translation.

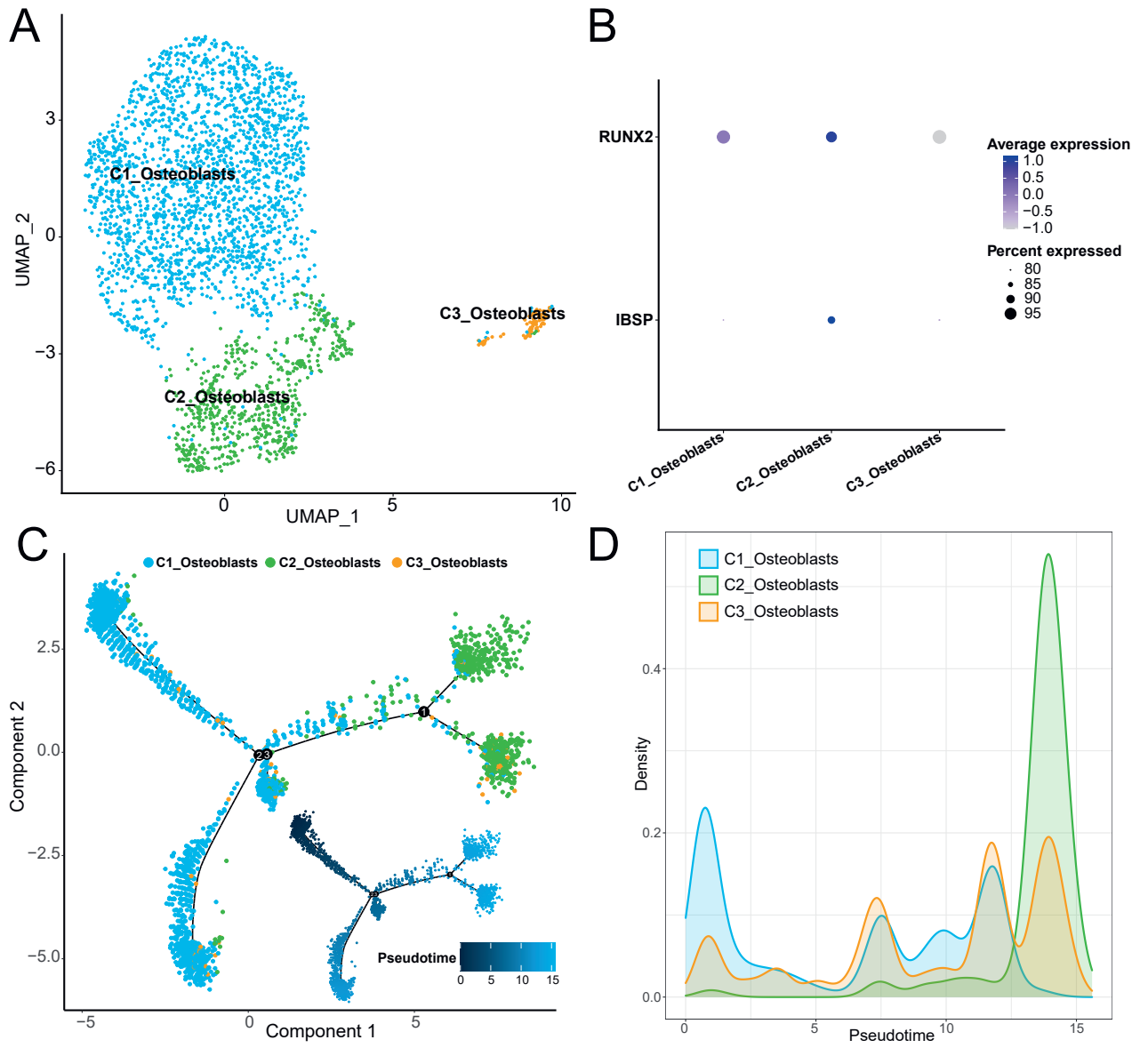

Fig. 2. The differentiation trajectory analysis of aneuploid osteoblasts in GCTB. (**A**) UMAP plot indicated the three main sub-clusters of aneuploid osteoblasts. (**B, C**) The monocle2 trajectory plot showing the differentiation trajectory of sub-clusters (**B**) and pseudotime curve (**C**). (**D**) The density plot of sub-clusters along pseudotime.

Pseudotime trajectory analysis of osteoclasts

It would be unconvincing if we only analysed the pseudotime trajectory of 119 aneuploid osteoclasts mentioned above. Thus, we analysed the pseudotime trajectory and sub-grouping of all osteoclasts (Fig. 4A–F). The results indicated that C1_Osteoclasts had high expression of mature osteoclast marker genes including *ACP5* and *CTSK*. The two marker genes were expressed at low levels in C2_Osteoclasts and not expressed in C3_Osteoclasts (Fig. 4B). These results suggested that C1_Osteoclasts are mature osteoclasts, C2_Osteoclasts are naive osteoclasts, and C3_Osteoclasts may be non-functioning osteoclasts. As shown in Fig. 4C–F, we found that osteoclasts followed the differentiation trajectory that began with the C2_Osteoclasts, which differentiated into C1_Osteoclasts. It is worth mentioning that most aneuploid osteoclasts belong to C1_Osteoclasts and C2_Osteoclasts, which existed in the end of the differentiation trajectory. All these results showed that the proportion of aneuploid cells gradually increased in GCTB with the differentiation and maturation of osteoclasts.

Moreover, we identified the DEGs between aneuploid and diploid osteoclasts (Fig. 4G). Interestingly, the up-regulated DEGs were mainly involved in biological functions such as proton transmembrane transport, ATP metabolic process and aerobic respiration (Fig. 4H), while down-regulated DEGs were mainly involved in the immune response, including activation of immune

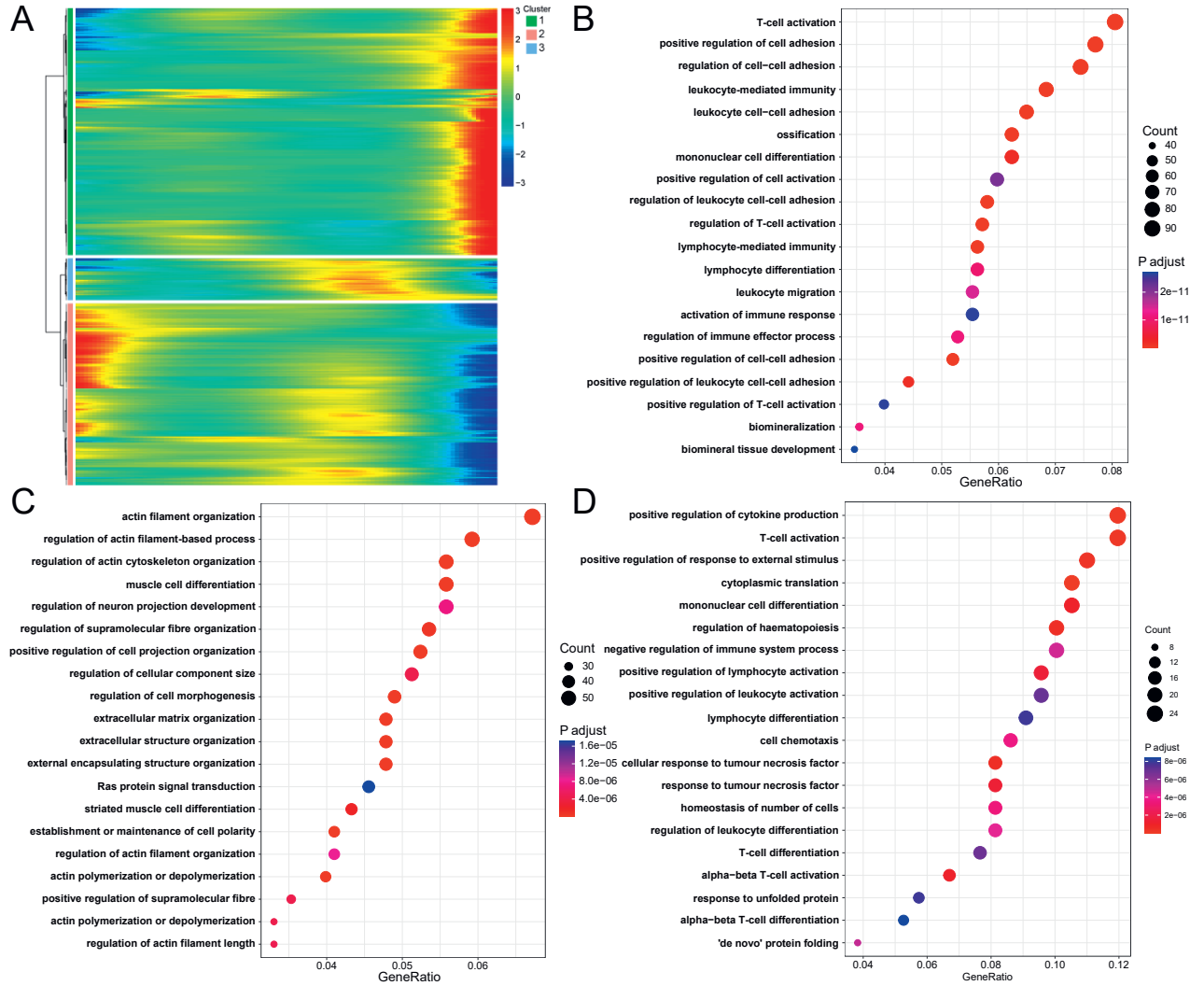

Fig. 3. The clustering and biological annotation of genes along the pseudotime. (**A**)The genes along the pseudotime were hierarchically clustered into three sub-clusters. (**B**) The top 15 biological process of genes in Cluster 1. (**C**) The top 15 biological process of genes in Cluster 2. (**D**) The top 15 biological process of genes in Cluster 3.

response, adaptive immune response based on somatic recombination of receptors and human immune response (Fig. 4I).

Furthermore, the genes changed with pseudotime were divided into four clusters. The gene expression value of Cluster 1 gradually decreased with the pseudotime. The gene expression value of Cluster 2 and Cluster 4 increased first and then decreased with the pseudotime and the gene expression value of Cluster 3 gradually increased with the pseudotime (Fig. 5A). Notably, we found that the genes in Cluster 1 were involved in the function of regulation of cell-cell adhesion (Fig. 5B). The Cluster 2 participated in T-cell activation and mononuclear cell differentiation (Fig. 5C). The genes in Cluster 3 were enriched in generation of precursor metabolites and energy, and the genes in Cluster 4 were related to the function of chromosome segregation and organelle fission (Fig. 5D–E). All the results suggested that the energy metabolism of osteoclasts gradually increased, and the biological functions of cell adhesion, cell proliferation and immune activation decreased during the process of maturation.

The cell-cell contact type of communication network in CellChat analysis

The CellChat analysis was performed to explore the cell-cell contact between aneuploid osteoblasts, osteoclasts and NK/T cells. As shown in Fig. 6A and 6B, the incoming and outgoing signalling pathways mainly interacted with aneuploid osteoblasts, suggesting that aneuploid osteoblasts played an important role in the immune microenvironment of GCTB. We also found that aneuploid osteoblasts might activate NK/T cells through antigen presentation via the MHC-I and MHC-II pathways. Interestingly, the results also indicated that aneu-

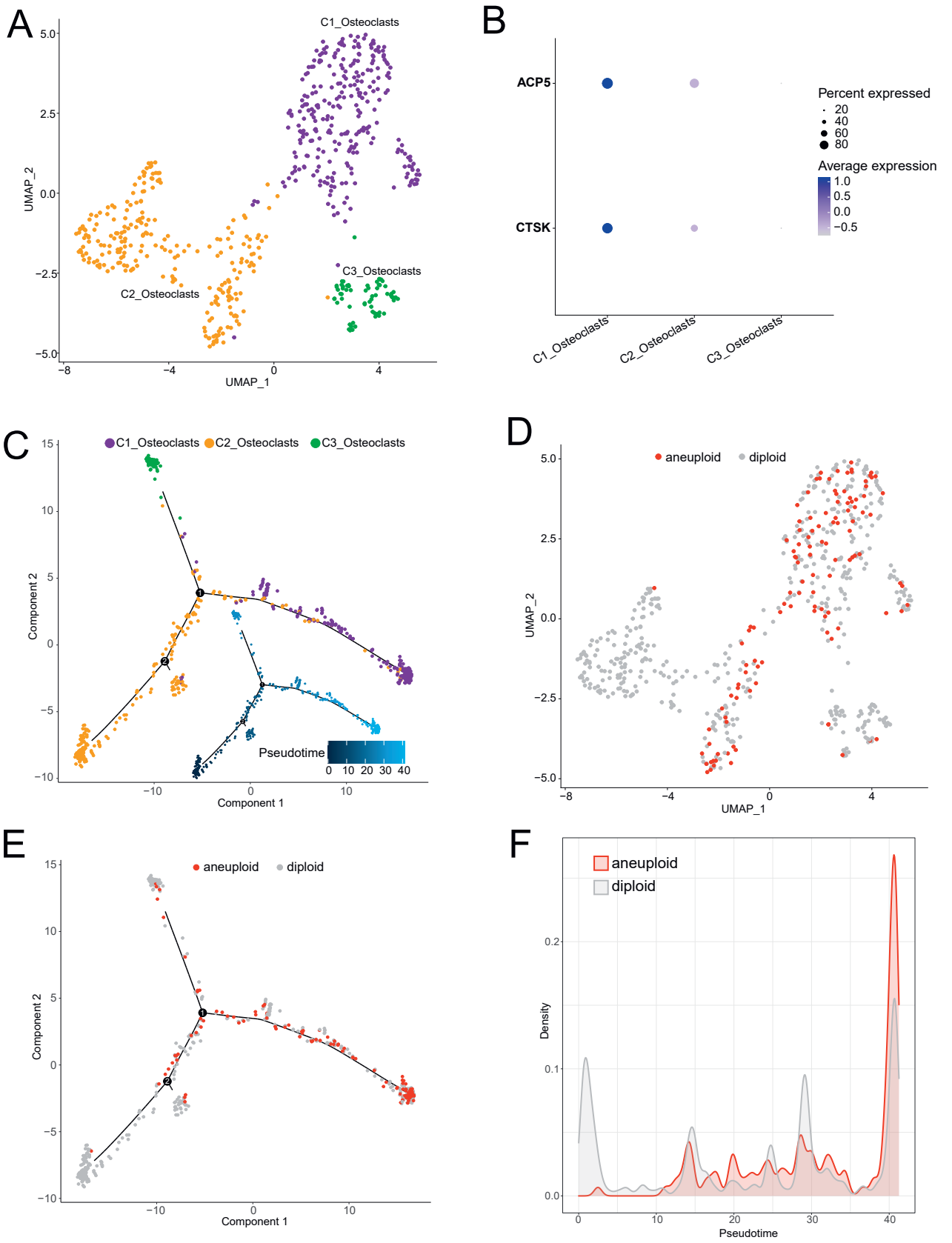

Fig. 4. The sub-clustering and trajectory analysis of osteoclasts in GTCB. (**A**) The UMAP plot shows the three main sub-clusters of osteoclasts. (**B**) The UMAP plot represents the distribution of aneuploid cells in osteoclasts. (**C, D, E**) The monocle2 trajectory plot showing the differentiation trajectory of sub-clusters (**C**), pseudotime curve (**D**), aneuploidy or diploidy (**E**). (**F**) The density plot of aneuploidy and diploidy along pseudotime.

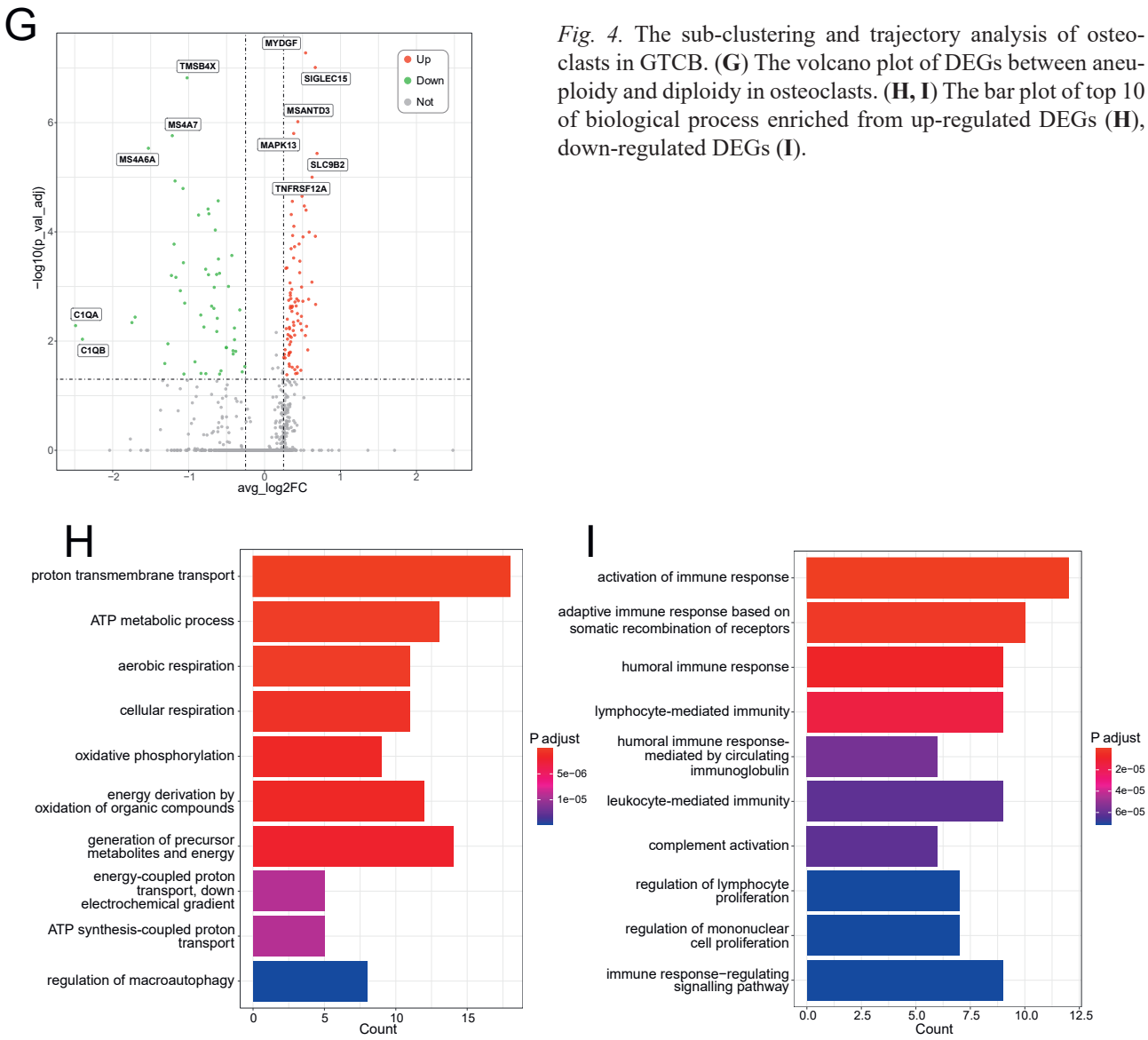

Fig. 4. The sub-clustering and trajectory analysis of osteoclasts in GTCB. (**G**) The volcano plot of DEGs between aneuploidy and diploidy in osteoclasts. (**H, I**) The bar plot of top 10 of biological process enriched from up-regulated DEGs (**H**), down-regulated DEGs (**I**).

ploid osteoclasts were involved in the TIGIT signalling pathway. Furthermore, the TIGIT signalling pathway was reported to be an important pathway for inhibiting immune cells, implying that aneuploid osteoclasts might suppress the activation of NK/T cells (Wang et al., 2021). Next, we identified the ligands/receptors between aneuploidy variant osteoblasts, osteoclasts and NK/T cells. We found that aneuploid osteoblasts activate NK/T cells through the antigen-presenting function of the HLA gene family. Aneuploid osteoclasts suppress NK/T cells via CD80-CTLA4 and CD86-CTLA4 (Fig. 6C–D).

The secreted signalling type of the communication network in CellChat analysis

We examined the secretory-type communication connections between aneuploid osteoblasts, osteoclasts and NK/T cells. Interestingly, we discovered that the majority of both incoming and outgoing signalling pathways originated from aneuploid osteoblasts. This finding suggests that aneuploid osteoblasts play a significant role in the communication dynamics of both cell contacts and secretory signals (Fig. 7A–D). We found that aneuploid osteoblasts act on NK/T cells through ligands MIF, PTN, GDF15, CD70, WNT5A, etc. Aneuploid osteoclasts act on NK/T cells through ligands TNFSF14, LGALS9, IL4, CCL5, etc. On the contrary, NK/T cells acted on aneuploid osteoblasts through ligands LTA, IFNG, GZMA, CCL5 and played a role in killing cells. NK/T cells act on aneuploid osteoclasts through ligands NRG1, CSF2, and CD40LG and also play a role in killing cells.

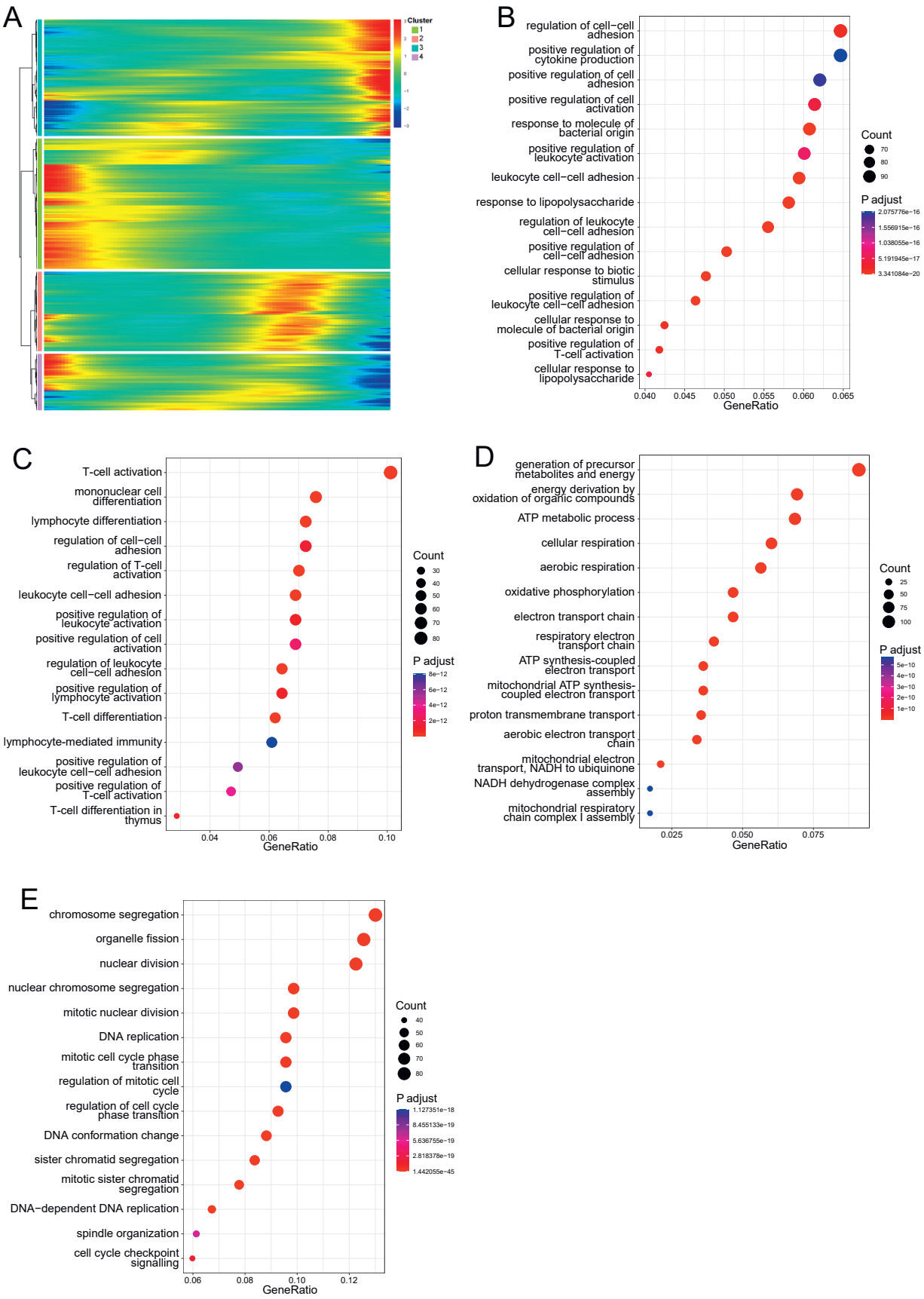

Fig. 5. The clustering and biological annotation of genes along the pseudotime. (**A**) The genes along the pseudotime were hierarchically clustered into four sub-clusters. (**B**) The top 15 biological process of genes in Cluster 1. (**C**) The top 15 biological process of genes in Cluster 2. (**D**) The top 15 biological process of genes in Cluster 3. (**E**) The top 15 biological process of genes in Cluster 4.

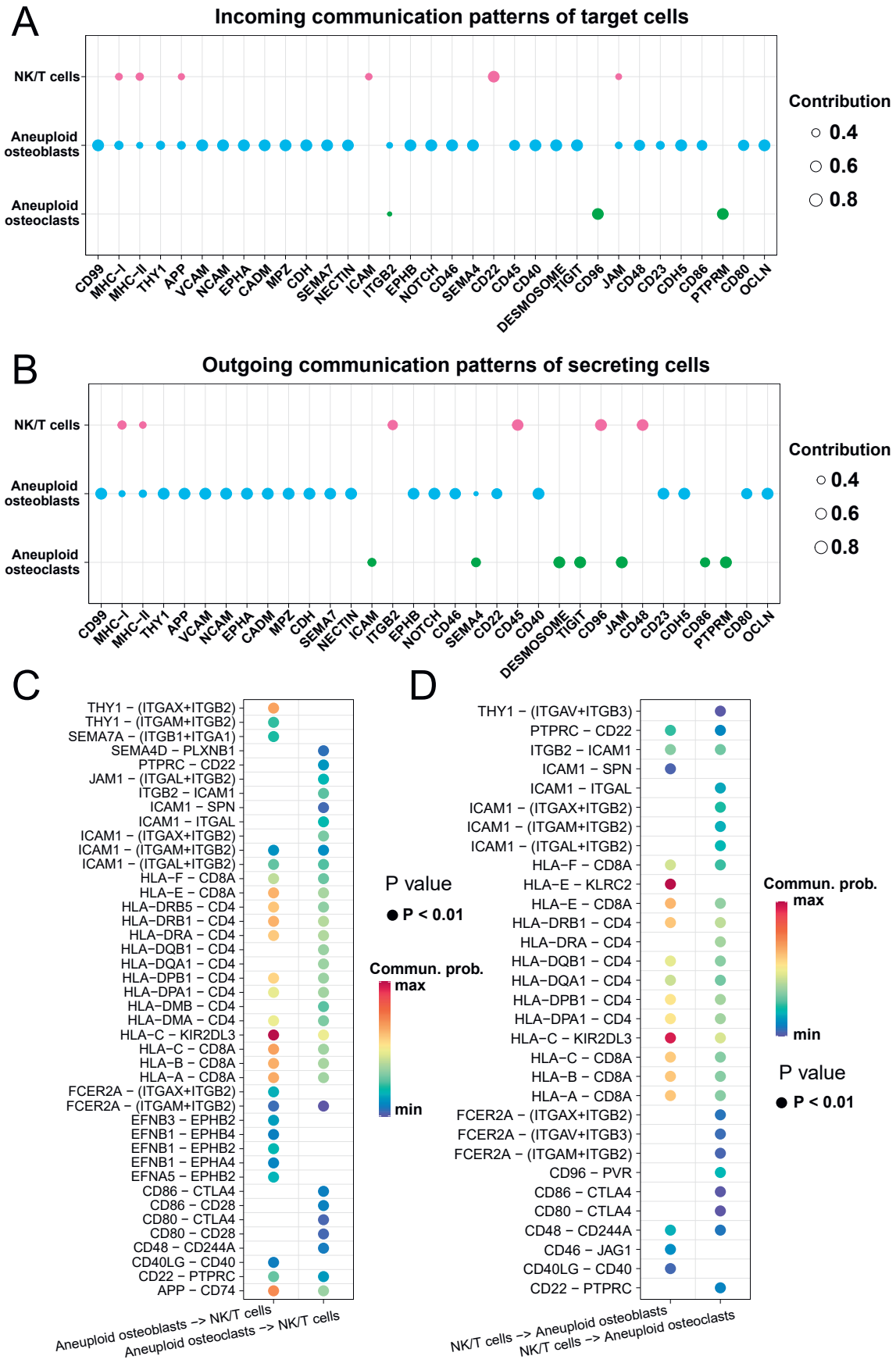

Fig. 6. The cell-cell contact type of communication network in CellChat analysis. (**A, B**) The bubble plot shows the incoming and outgoing communication signalling pathways of aneuploid osteoblasts, aneuploid osteoclasts and NK/T cells. (**C, D**) The bubble plot indicates the ligand-receptor pairs that have known biological significance.

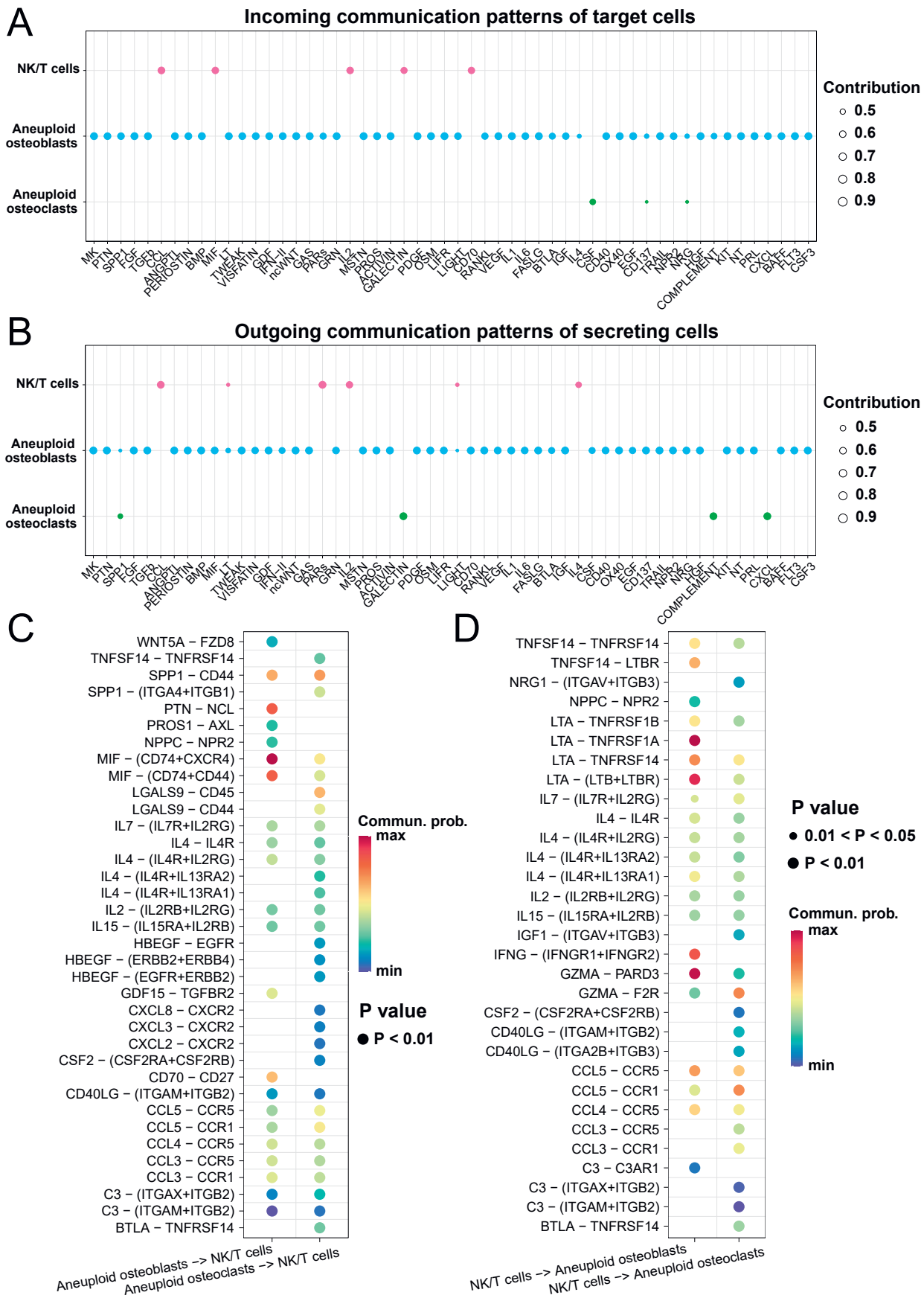

Fig. 7. The secreted signalling type of communication network in CellChat analysis. (**A, B**) The bubble plot shows the incoming and outgoing communication signalling pathways of aneuploid osteoblasts, aneuploid osteoclasts and NK/T cells. (**C, D**) The bubble plot shows the ligand-receptor pairs that have known biological significance

Discussion

GCTB is a giant cell-rich bone lesion. Previous studies have indicated that the giant cells mainly included osteoclasts (Feng et al., 2021; Lan et al., 2022). Some drugs, such as denosumab and zoledronic acid, could reduce the differentiation of osteoclasts from mononuclear cells including osteoclast precursors (Shibuya et al., 2019). However, recent studies reported that osteoblasts might be the origin of GCTB. Feleke et al. (2022) found that eight cell types were identified by unique marker genes, which included osteoblasts. Thus, in our study, we first found that most aneuploid cells were osteoblasts in patients with GCTB. Then, we explored the function and differentiation trajectory of osteoblasts in GCTB. Moreover, we identified the aneuploid cells in GCTB and analysed their function in the development of GCTB.

Aneuploid cells are the hallmark of cancers, providing a promising chance for treating cancers and strategies of prevention (Tang et al., 2017; Cohen-Sharir et al., 2021). In our study, we identified the aneuploid cells in GCTB, suggesting that most aneuploid cells were osteoblasts. Further analysis showed that aneuploid osteoblasts first promote the inflammatory response activity, and then enhance the ability to activate T cells, while biological functions such as cell morphogenesis, extracellular matrix and actin fibre organization decline. The results indicated that osteoblasts might be the main reasons for processes occurring in GCTB; further experiments need to be performed to validate these results. Meanwhile, we also analysed the function of aneuploid osteoclasts, indicating that these cells increase the energy metabolism capacity of cells and weaken the immune response when compared with diploid cells. This result also showed that aneuploid osteoclasts inhibited the immune function, which was consistent with the results from previous study. Elsayed et al. (2020) believed that aneuploid osteoclasts lead to impaired immune functions such as differentiation, maturation, migration, antigen presentation, as well as activation of T cells. At the same time, this study also found that the cellular energy metabolism response is gradually enhanced, and the biological functions of cell adhesion, cell proliferation and immune activation are gradually weakened during the process of differentiation and maturation of osteoclasts in GCTB. This finding is consistent with the results of the differential expression analysis and functional annotation of aneuploid osteoclasts and diploid osteoclasts described above.

Furthermore, in our study, the analysis of communication connections indicated that aneuploid osteoclasts were involved in the signalling pathways including TIGIT, which is the key pathway for inhibiting the immune response. This result suggested that aneuploid osteoclasts played a novel role in suppression of the NK/T-cell function. Besides, we also found that aneuploid osteoclasts suppressed NK/T cells via CD80-CTLA4 and CD86-CTLA4. These results implied that blocking CTLA4 or TIGIT with the immune checkpoint blockade could attenuate the inhibitory effect of aneuploid osteoclasts on NK/T cells, thereby enhancing the NK/T-cell activity. *TIGIT* and *CTLA4* are important immune checkpoint genes, which are mainly expressed on immune cells, including NK cells, T cells and other antigen-presenting cells; they were found to diminish production of cytokines and exhibit intense inhibition features (de Vos et al., 2022). TIGIT is a molecule that inhibits lymphocyte expression and negatively regulates the T-cell function (Kurtulus et al., 2015). Meanwhile, Zheng et al. (2020) found that TIGIT could achieve an active anti-tumour immune response and play a vital role in immunotherapy for cancers. Besides, CTLA4 can attenuate T-cell activation by inhibiting co-stimulation and transmitting inhibitory signals to T cells (Adams et al., 2016). Feleke et al. (2022) found that EGFL7, VEGF-A-D and TNFSF11 show considerable cell-to-cell variability in OS and GCTB; the activity of these genes likely plays a role in the heterogeneity in these cancers and could be essential for tumour progression, metastasis, and disease recurrence in OS and GCTB. So far, few studies have reported that the two immune checkpoint genes, *TIGIT* and *CTLA4*, might be the key biomarkers for GCTB, which provides novel directions in the therapies of patients with GCTB.

Conclusion

In summary, in this study we have further explored the heterogeneity of GCTB and identified that most aneuploid cells were osteoblasts in the patients with GCTB. We also analysed the function of osteoblasts and osteoclasts, indicating that both of them might be involved in the process of GCTB. We also provided a novel direction for treating GCTB.

Availability of data and materials

The datasets generated and/or analysed during the current study are available in the Gene Expression Omnibus (GEO) repository, https://www.ncbi.nlm.nih.gov/geo/query/acc.cgi?acc=GSE168664 .

Competing interests

The authors declare that they have no competing interests.

Author contributions

Bohua Gao: conceptualization, writing – original draft, writing – review and editing. Yan Wang: data curation, formal analysis. Ye Zhang and Zhongren Chen: investigation, validation. Guangfu Ming: writing – original draft, writing – review and editing.

References

Adams, A. B., Ford, M. L., Larsen, C. P. (2016) Costimulation blockade in autoimmunity and transplantation: the CD28 pathway. *J. Immunol.* **197**, 2045-2050.

Auvinen, K., Lokka, E., Mokkala, E. et al. (2019) Fenestral diaphragms and PLVAP associations in liver sinusoidal endothelial cells are developmentally regulated. *Sci. Rep.* **9**, 15698.

Azizi, E., Carr, A. J., Plitas, G. et al. (2018) Single-cell map of diverse immune phenotypes in the breast tumour microenvironment. *Cell* **174**, 1293-1308.e1236.

Baird, A., Lindsay, T., Everett, A. et al. (2018) Osteoblast differentiation of equine induced pluripotent stem cells. *Biol. Open* **7**, bio033514.

Cohen-Sharir, Y., McFarland, J. M., Abdusamad, M. et al. (2021) Aneuploidy renders cancer cells vulnerable to mitotic checkpoint inhibition. *Nature* **590**, 486-491.

Chen, J., Chen, F., Bian, H. et al. (2019) Hypertrophic chondrocyte-specific Col10a1 controlling elements in Cre recombinase transgenic studies. *Am. J. Transl. Res.* **11**, 6672-6679.

Chen, Y. P., Yin, J. H., Li, W. F. et al. (2020) Single-cell transcriptomics reveals regulators underlying immune cell diversity and immune subtypes associated with prognosis in nasopharyngeal carcinoma. *Cell Res.* **30**, 1024-1042.

Chim, S. M., Qin, A., Tickner, J. et al. (2011) EGFL6 promotes endothelial cell migration and angiogenesis through the activation of extracellular signal-regulated kinase. *J. Biol. Chem.* **286**, 22035-22046.

Clark, B. S., Stein-O'Brien, G. L., Shiau, F. et al. (2019) Single-cell RNA-Seq analysis of retinal development identifies NFI factors as regulating mitotic exit and late-born cell specification. *Neuron* **102**, 1111-1126.e5.

de Vos, L., Carrillo Cano, T. M., Zarbl, R. et al. (2022) CTLA4, PD-1, PD-L1, PD-L2, TIM-3, TIGIT, and LAG3 DNA methylation is associated with BAP1-aberrancy, transcriptional activity, and overall survival in uveal melanoma. *J. Immunother*. **45**, 324-334

Elsayed, R., Kurago, Z., Cutler, C. W. et al. (2020) Role of dendritic cell-mediated immune response in oral homeostasis: a new mechanism of osteonecrosis of the jaw. *FASEB J.* **34**, 2595-2608.

Feleke, M., Feng, W., Song, D. et al. (2022) Single-cell RNA sequencing reveals differential expression of EGFL7 and VEGF in giant-cell tumour of bone and osteosarcoma. *Exp. Biol. Med. (Maywood)* **247**, 1214-1227.

Feng, W., He, M., Jiang, X. et al. (2021) Single-cell RNA sequencing reveals the migration of osteoclasts in giant cell tumour of bone. *Front. Oncol.* **11**, 715552.

Gao, R., Bai, S., Henderson, Y. C. et al. (2021) Delineating copy number and clonal substructure in human tumours from single-cell transcriptomes. *Nat. Biotechnol.* **39**, 599-608.

Giesche, J., Mellert, K., Geißler, S. et al. (2022) Epigenetic lockdown of CDKN1A (p21) and CDKN2A (p16) characterises the neoplastic spindle cell component of giant cell tumours of bone. *J. Pathol*. **257**, 687-696.

Ji, Z., Chuen, J., Kiparaki, M. et al. (2021) Cell competition removes segmental aneuploid cells from Drosophila imaginal disc-derived tissues based on ribosomal protein gene dose. *Elife* **10**, e61172.

Jin, S., Guerrero-Juarez, C. F., Zhang, L. et al. (2021) Inference and analysis of cell-cell communication using CellChat. *Nat. Commun.* **12**, 1088.

Kurtulus, S., Sakuishi, K., Ngiow, S. F. et al. (2015) TIGIT predominantly regulates the immune response via regulatory T cells. *J. Clin. Invest.* **125**, 4053-4062.

Lan, Z., Wang, T., Zhang, L. et al. (2022) CircSLC8A1 exacerbates hypoxia-induced myocardial injury via interacting with miR-214-5p to upregulate TEAD1 expression. *Int. Heart J.* **63**, 591-601.

Lee, H. W., Chung, W., Lee, H. O. et al. (2020) Single-cell RNA sequencing reveals the tumour microenvironment and facilitates strategic choices to circumvent treatment failure in a chemorefractory bladder cancer patient. *Genome Med.* **12**, 47.

Li, H., Gao, J., Gao, Y. et al. (2020) Denosumab in giant cell tumour of bone: current status and pitfalls. *Front. Oncol.* **10**, 580605.

Liu, T., Zhang, H., Yi, S. et al. (2019) Mutual regulation of MDM4 and TOP2A in cancer cell proliferation. *Mol. Oncol.* **13**, 1047-1058.

Mereu, E., Lafzi, A., Moutinho, C. et al. (2020) Benchmarking single-cell RNA-sequencing protocols for cell atlas projects. *Nat. Biotechnol.* **38**, 747-755.

Moskovszky, L., Szuhai, K., Krenács, T. et al. (2009) Genomic instability in giant cell tumour of bone. A study of 52 cases using DNA ploidy, relocalization FISH, and array-CGH analysis. *Genes Chromosomes Cancer* **48**, 468-479.

Nordstrand, A., Bovinder Ylitalo, E., Thysell, E. et al. (2018) Bone cell activity in clinical prostate cancer bone metastasis and its inverse relation to tumour cell androgen receptor activity. *Int. J. Mol. Sci.* **19**, 1223.

Peng, J., Sun, B. F., Chen, C. Y. et al. (2019) Single-cell RNA-seq highlights intra-tumoural heterogeneity and malignant progression in pancreatic ductal adenocarcinoma. *Cell Res.* **29**, 725-738.

Qiu, X., Mao, Q., Tang, Y. et al. (2017) Reversed graph embedding resolves complex single-cell trajectories. *Nat. Methods* **14**, 979-982.

Sbaraglia, M., Bellan, E., Dei Tos, A. P. (2021) The 2020 WHO Classification of Soft Tissue Tumours: news and perspectives. *Pathologica* **113**, 70-84.

Shibuya, I., Takami, M., Miyamoto, A. et al. (2019) In vitro study of the effects of denosumab on giant cell tumour of bone: comparison with zoledronic acid. *Pathol. Oncol. Res.* **25**, 409-419.

Tang, Y. C., Yuwen, H., Wang, K. et al. (2017) Aneuploid cell survival relies upon sphingolipid homeostasis. *Cancer Res.* **77**, 5272-5286.

Tirosh, I., Izar, B., Prakadan, S. M. et al. (2016a) Dissecting the multicellular ecosystem of metastatic melanoma by single-cell RNA-seq. *Science* **352**, 189-196.

Tirosh, I., Venteicher, A. S., Hebert, C. et al. (2016b) Single-cell RNA-seq supports a developmental hierarchy in human oligodendroglioma. *Nature* **539**, 309-313.

van der Heijden, L., Dijkstra, S., van de Sande, M. et al. (2020) Current concepts in the treatment of giant cell tumour of bone. *Curr. Opin. Oncol.* **32**, 332-338.

Wang, J., Hou, H., Mao, L. et al. (2021) TIGIT signaling pathway regulates natural killer cell function in chronic hepatitis B virus infection. *Front. Med. (Lausanne)* **8**, 816474.

Yao, Z. P., Zhu, H., Shen, F. et al. (2022) Hsp90 regulates the tumourigenic function of tyrosine protein kinase in osteosarcoma. *Clin. Exp. Pharmacol. Physiol.* **49**, 380-390.

Zhang, X., Lan, Y., Xu, J. et al. (2019) CellMarker: a manually curated resource of cell markers in human and mouse. *Nucleic Acids Res.* **47**, D721-D728.

Zheng, Q., Xu, J., Gu, X. et al. (2020) Immune checkpoint targeting TIGIT in hepatocellular carcinoma. *Am. J. Transl. Res.* **12**, 3212-3224.

Zhou, Y., Yang, D., Yang, Q. et al. (2020) Single-cell RNA landscape of intratumoural heterogeneity and immunosuppressive microenvironment in advanced osteosarcoma. *Nat. Commun.* **11**, 6322.